LA-UR-17-29182
Approved for public release; distribution is unlimited.

Title: A New Multiphase Equation of State for SiO2

Author(s): Maerzke, Katie A.
Gammel, J. Tinka

Intended for: Report

Issued: 2017-10-06

A New Multiphase Equation of State for SiO_2

Katie A. Maerzke and J. Tinka Gammel
*Theoretical Division, Los Alamos National Laboratory, Los Alamos, NM 87545**

(Dated: October 5, 2017)

I. INTRODUCTION

SiO_2 is found as α-quartz at ambient conditions. Under shock compression, it transforms into a much higher density stishovite-like phase around 20 GPa, then into a liquid phase above 100 GPa. The SESAME library contains older equations of state for α-quartz, polycrystalline quartz, and fused quartz. These equations of state model the material as a single phase; i.e., there is no high pressure phase transition. Somewhat more recently (in 1992), Jon Boettger published equations of state for α-quartz, coesite, and stishovite, along with a phase transition model to mix them [1]. However, we do not have a multiphase EOS that captures the phase transitions in this material. Others are working on a high-accuracy model for very high pressure SiO_2, since liquid quartz is used as an impedance matching standard above 100 GPa; however, we are focused on the $10 - 50$ GPa range. This intermediate pressure range is most relevant for modeling the decomposition products of silicone polymers such as Sylgard 184 and SX358.

II. EQUATION OF STATE MODEL

A chemically inert multiphase equation of state (EOS) was constructed using the SESAME model [2], in which the the Helmholtz free energy F is expressed as a three-part decomposition,

$$F(\rho, T) = F_{\text{cold}}(\rho) + F_{\text{ionic}}(\rho, T) + F_{\text{elec}}(\rho, T) \tag{1}$$

as a function of density ρ and temperature T. The first term represents the cold curve, or the free energy of the electronic ground state with the ions in their equilibrium configuration (which does not include zero point energy). The second term describes the ionic motion in the ground electronic state, and the third term the electronic excitations. Electronic excitations, which are generally negligible, were calculated using the Thomas-Fermi-Dirac model [3].

Analogous to carbon models (graphite and diamond) in thermochemical codes, we have chosen to model SiO_2 as a low-pressure α-quartz phase and a high-pressure stishovite-like phase.

*Electronic address: kmaerzke@lanl.gov

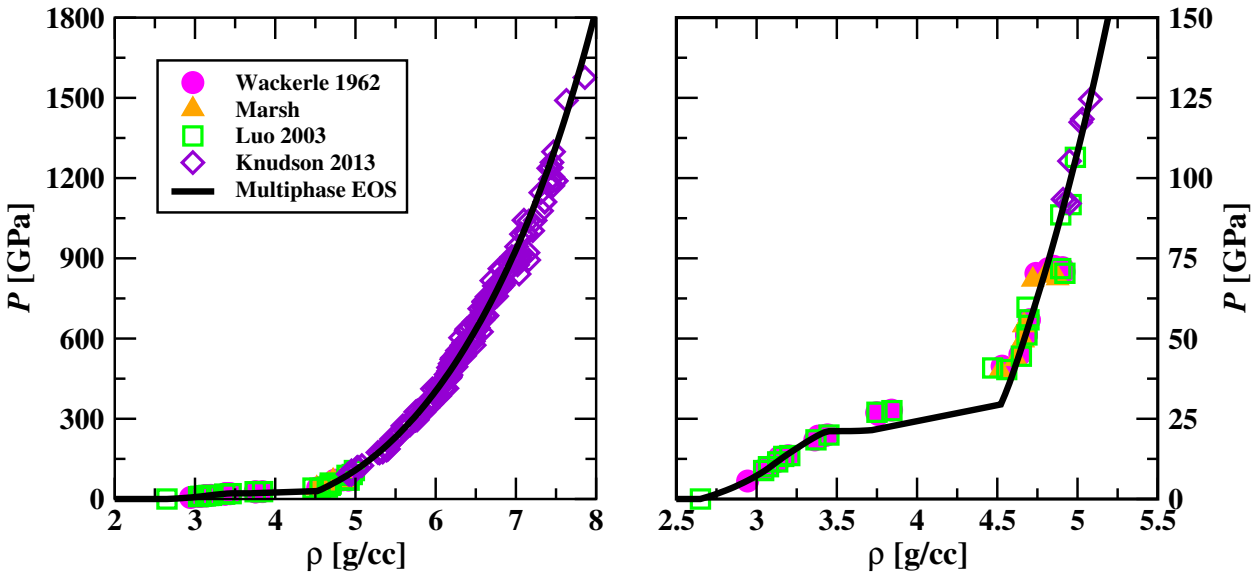

FIG. 1: $P-\rho$ Hugoniot plots. Experimental data (symbols) and multiphase EOS (black line). Wackerle [13] magenta circles, Marsh [14] orange triangles, Luo [9] green squares, and Knudson [15] violet diamonds. Note that Luo et al. cite Wackerle 1962, but Luo et al. exlude the data points that appear to be outliers and include others of unknown origin. The right panel is a zoomed-in version of the left panel that focuses on the phase transition.

There is a clear change in density on the Hugoniot above approximately 20 GPa, which is attributed to a phase change from α-quartz to a higher density material, likely stishovite. Experiments to determine the identity of the high pressure phase have yielded contradictory results, though it seems likely to be stishovite [4–10]. Some shock data where SiO_2 is initially stishovite, rather than quartz, exists [11, 12]; however, we have not attempted to model that with our EOS. Given the uncertainty surrounding the identity of the high-pressure phase of SiO_2 shocked from α-quartz, along with the unknown dynamic effects that could vary when shocking stishovite vs. α-quartz, we believe this is a reasonable decision. Furthermore, many more polymorphs of SiO_2 exist, such as coesite, cristobalite, and β-quartz; however, these phases are not formed during the shock compression of α-quartz (to the best of our knowledge). Thus, attempting to include all of these phases in our multiphase EOS would only cause unnecessary complications.

The α-quartz EOS is the Boettger EOS from 1992 [1] with a few small changes. The cold curve was fit to shock data in the $U_\mathrm{s} - u_\mathrm{p}$ plane using the equation

$$U_\mathrm{S} = c_0 + s_1 u_\mathrm{p} \tag{2}$$

In this updated EOS, we have changed s_1 from 1.75 to 1.907, which results in a change in $\mathrm{d}B_S/\mathrm{d}P$ from 6.0 to 6.628 (using the ambient relation $4s_1 - 1 = \mathrm{d}B_S/\mathrm{d}P$). Experimental measurements of

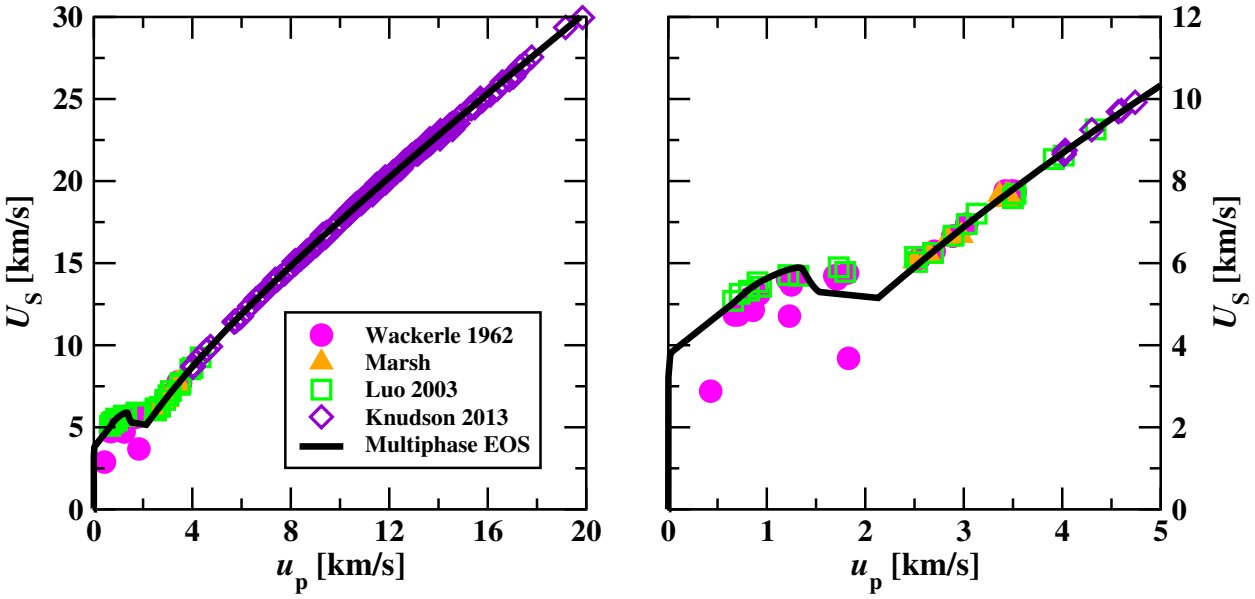

FIG. 2: $U_S - u_p$ Hugoniot plots. Experimental data (symbols) and multiphase EOS (black line). Wackerle [13] magenta circles, Marsh [14] orange triangles, Luo [9] green squares, and Knudson [15] violet diamonds. Note that Luo et al. cite Wackerle 1962, but Luo et al. exlude the data points that appear to be outliers and include others of unknown origin. The right panel is a zoomed-in version of the left panel that focuses on the phase transition.

$\mathrm{d}B/\mathrm{d}P$ vary from 4.7 to 6.7 [16–18], with an average of about 6. However, the slightly larger value gives us a better fit to the data, and is in agreement with the most recent measurement of 6.7 [18]. We also changed the nuclear model from the older chartjd to the newer hightliq [19, 20], which works better with the multiphase construction in OpenSesame [21]. The α-quartz EOS was used as a starting point for the high-pressure stishovite-like phase, but significant changes were required. The cold model was changed to finite_strain [19, 22, 23] with a coefficient of -500 to improvement agreement with the very high pressure liquid SiO_2 data. The bulk modulus for the stishovite-like phase is set to 300 GPa, which is much higher than the value for quartz (37.7 GPa, using $B_S = c_0^2\rho_0$), somewhat smaller than the value used by Boettger ($\approx$ 350 GPa), but in good agreement with the average experimental value for stishovite [16, 17, 24]. We have increased $\mathrm{d}B_S/\mathrm{d}P$ from the value of 3 used by Boettger to 6.0, which gives us a better fit to the higher pressure α-quartz shock data. Experimental measurements of $\mathrm{d}B/\mathrm{d}P$ for stishovite vary considerably, ranging from 0.7 to 6.9 [16, 17, 24]; thus, both 3 and 6 are reasonable values. The Grüneisen Γ was increased from 0.65 for α-quartz to 1.25 for the high-pressure stishovite-like phase. All input parameters can be found in the Appendix. One of us (JTG) modified the OpenSesame multiphase algorithm to handle the large volume difference between the phases. Minimal "windowing" was used to enforce the correct phase boundaries; the only window parameter is a maximum quartz density to prevent re-entrant behavior at very high densities.

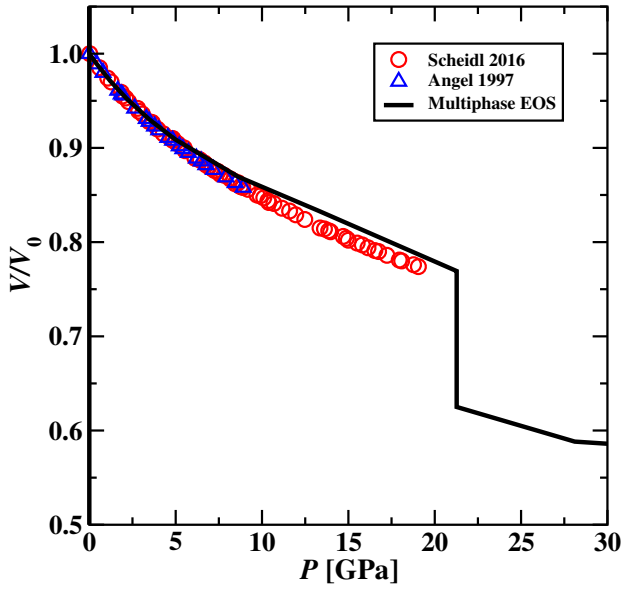

FIG. 3: Hydrostatic compression data for α-quartz from diamond anvil cell experiments at 298 K. Data from Angel et al. [25] (blue triangles) and Scheidel et al. [18] (red circles), and the new multiphase EOS (black solid line). Note the phase change in the EOS to the stishovite-like material around 20 GPa.

III. RESULTS AND DISCUSSION

Figures 1 and 2 show excellent agreement between the available shock data and the new multiphase EOS. There is a small amount of noise in the transition region, especially noticeable around $u_{\rm p} = 1.5$ km/s, which is due to the limitations of the Hugoniot solver. Above approximately 100 GPa there is another phase transition from solid to liquid, which we are not modeling with a separate liquid EOS. Instead, we use the hightliq nuclear model [19, 20] where the EOS transitions to a liquid-like model above $T_{\rm melt}$. This, coupled with the finite_strain coefficient of -500, allows us to capture the very high pressure data quite well.

In addition to shock data, we have some hydrostatic compression and thermal data for α-quartz. In Figure 3 we find excellent agreement with data below about 5 GPa. Above 5 GPa the agreement is still good, though the EOS predicts that the material is slightly less compressible. A clear transition to the high-pressure stishovite-like phase can be seen at 21 GPa. Our new multiphase EOS shows good agreement with the heat capacity data, as can be seen in Figure 4. The experimental data show a phase transition to β-quartz at 847 K, which we are not attempting to model with our EOS (β-quartz does not appear in shock compression experiments). At 1 atm and $T \leq 2000$ K our EOS predicts that the material is α-quartz. We also have data for the coefficient of thermal expansion (α, see Figure 5), though there is less agreement between different experimental

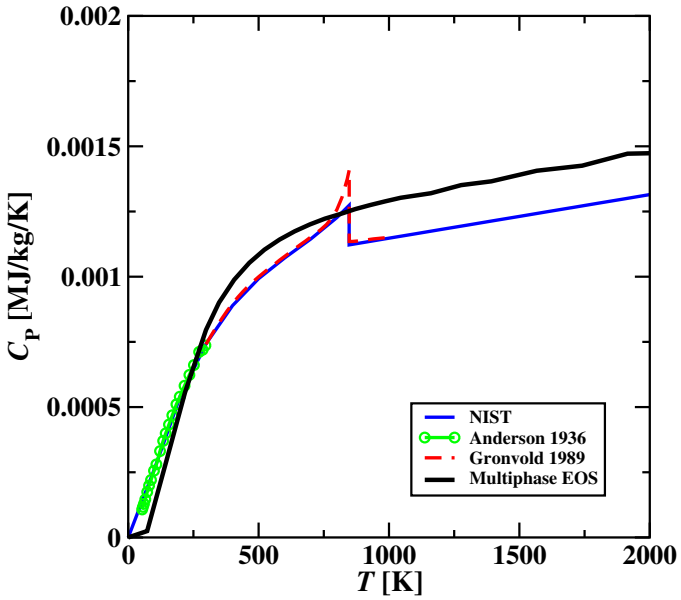

FIG. 4: Plot showing C_P at 1 atm as a function of temperature. NIST data [26] (blue solid line), Anderson [27] (green circles), Grønvold [28] (red dashed line), and the new multiphase EOS (black solid line). Note that the transition at 847 K is the α to β quartz transition, which we are not attempting to model with this EOS.

sources. Our EOS is able to capture the trend in the data reasonably well, with very small values of α across the temperature range where we have data.

By examining the phase diagrams (see Figures 6, 7, 8) we can see that the new multiphase EOS is generally well-behaved, without any high pressure or high density re-entrant behavior. We do see a small amount of the stishovite-like phase at low pressure and high temperature (see Figure 6) and low density and high temperature (see Figure 7). This could be eliminated by windowing (e.g., a minimum allowed density for the stishovite-like phase), but that will introduce discontinuities into the table, which creates problems when attempting to use the EOS in a hydrodynamics simulation. Since this is a part of phase space that is extremely unlikely to be accessed in any shock compression simulation, the choice to either leave the re-entrant behavior or use windowing is unimportant. In Figure 8 we have plotted the Hugoniot on top of the phase boundaries, which shows that at each point along the Hugoniot the material exists in the correct phase. Though our phase boundaries are reasonable, we do not reproduce the experimental SiO_2 phase diagram. Real SiO_2 can be found in many other phases (coesite, crisobalite, β-quartz, etc.) which we are not attempting to model. These phases are not relevant for the shock compression of α-quartz and would unnecessarily complicate our modeling efforts.

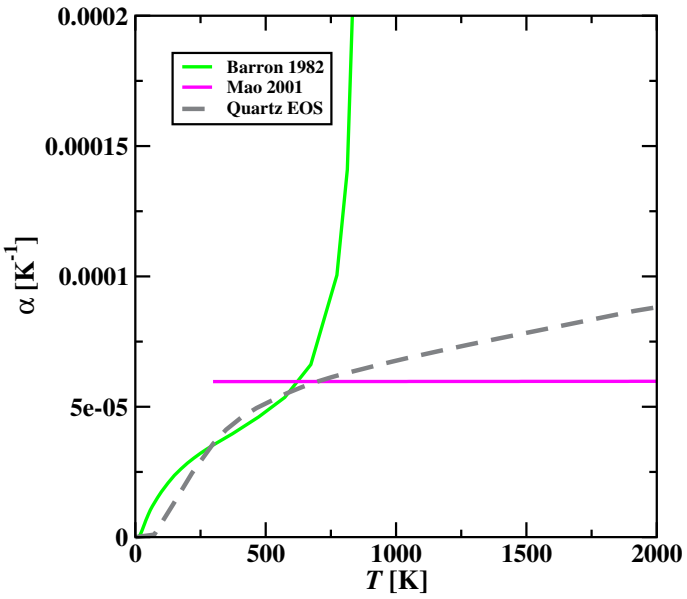

FIG. 5: Plot showing the coefficient of thermal expansion (α) at 1 atm as a function of temperature. Barron [29] (green line), Mao [17] (magenta line), and the quartz EOS (dashed gray line). Note that the OpenSesame interpolator has trouble with the coefficient of thermal expansion when using the 311 tables, which results in a very noisy curve for the multiphase EOS (not shown).

IV. CONCLUSIONS

Our new multiphase SiO_2 equation of state accurately models the phase transition seen in α-quartz under shock compression, with a stishovite-like high-pressure phase. We also obtain good agreement with the very high pressure data (above 100 GPa), though this was not our area of focus. This is an improvement over the SiO_2 equations of state currently available in the SESAME library, where the material is modeled as a single phase. This new multiphase SiO_2 EOS is suitable for use in thermochemical modeling of the decomposition products of silicone polymers.

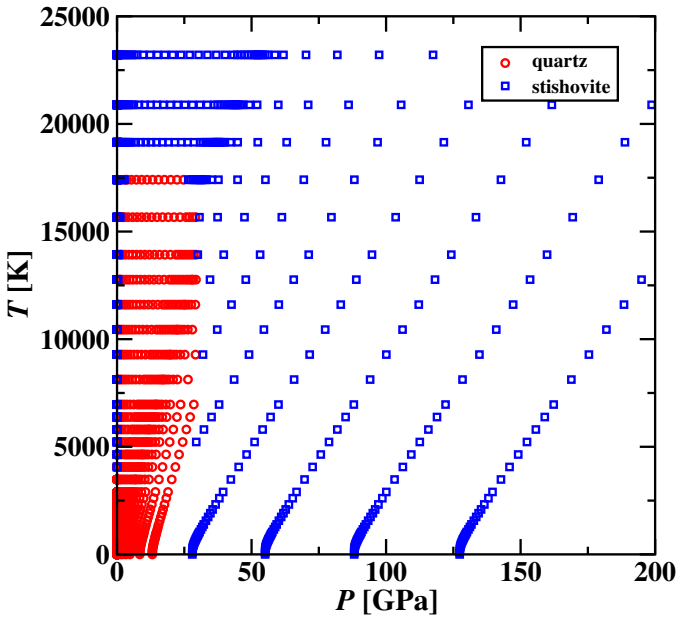

FIG. 6: $P-T$ phase diagram showing which regions of phase space are α-quartz (red circles) and which are stishovite-like (blue squares).

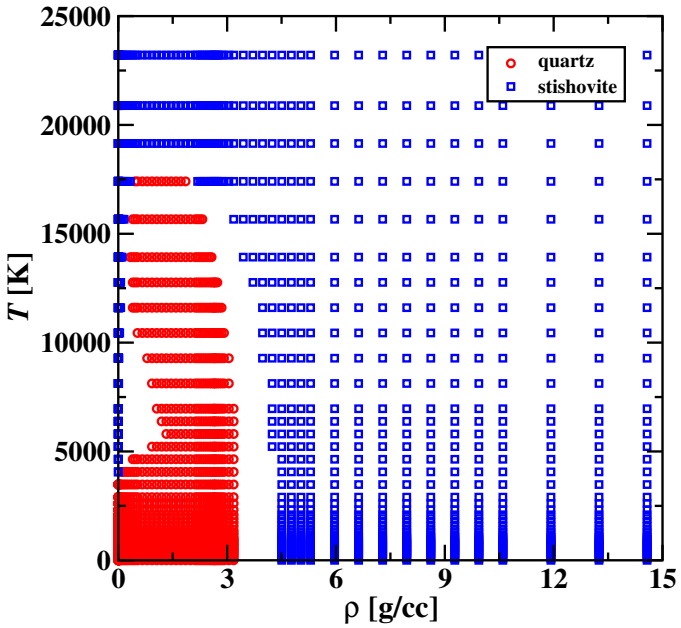

FIG. 7: $\rho-T$ phase diagram showing which regions are α-quartz (red circles) and which are stishovite-like (blue squares).

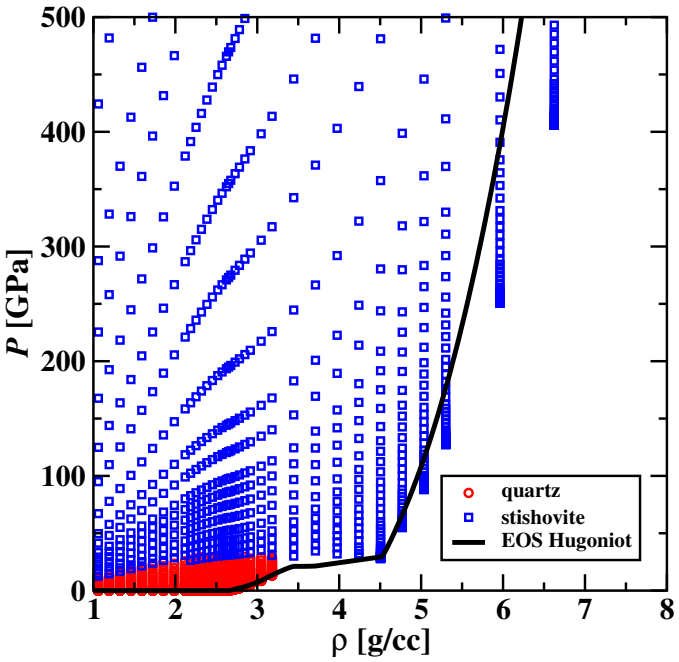

FIG. 8: $\rho - P$ phase diagram showing which regions are α-quartz (red circles) and which are stishovite-like (blue squares). The black line is the $P(\rho)$ Hugoniot from the new multiphase EOS. The high density and low pressure region does not contain data points as that is outside the modeled region.

References

[1] J. C. Boettger, J. Appl. Phys. **72**, 5500 (1992).

[2] S. P. Lyon and J. D. Johnson, Tech. Rep. LA-UR-92-3407, Los Alamos National Laboratory Technical Report (1992).

[3] R. G. Parr and W. Yang, *Density-Functional Theory of Atoms and Molecules* (Oxford University Press, New York, NY, 1989).

[4] P. S. D. Carli and D. J. Milton, Science **147**, 144 (1965).

[5] J. D. Kleeman and T. J. Ahrens, J. Geophys. Res. **78**, 5954 (1973).

[6] D. E. Grady, W. J. Murri, and G. R. Fowles, J. Geophys. Res. **79**, 332 (1974).

[7] Y. Tsuchida and T. Yagi, Nature **340**, 217 (1989).

[8] J. A. Akins and T. J. Ahrens, Geophys. Res. Lett. **29**, 1394 (2002).

[9] S.-N. Luo and T. J. Ahrens, J. Geophys. Res. **108**, 2421 (2003).

[10] O. Tschauner, S.-N. Luo, P. D. Asimow, and T. J. Ahrens, Am. Mineral. **91**, 1857 (2006).

[11] S.-N. Luo, J. L. Mosenfelder, P. D. Asimow, and T. J. Ahrens, Geophys. Res. Lett. **29**, 36 (2002).

[12] M. Millot, N. Dubrovinkskaia, A. Černok, S. Blaha, L. Dubrovinsky, D. G. Braun, P. M. Celliers, G. W. Collins, J. H. Eggert, and R. Jeanloz, Science **347**, 418 (2015).

[13] J. Wackerle, J. Appl. Phys. **33**, 922 (1962).

[14] S. P. Marsh, *LASL Shock Hugoniot Data* (University of California Press, Berkeley, CA, 1980).

[15] M. D. Knudson and M. P. Desjarlais, Phys. Rev. B **88**, 184107 (2013).

[16] L.-G. Liu, Mech. Mater. **14**, 283 (1993).

[17] H. Mao, B. Sundman, Z. Wang, and S. K. Saxena, J. Alloys Compd. **327**, 253 (2001).

[18] K. S. Scheidl, A. Kurnosov, D. M. Trots, T. B. Ballaran, R. J. Angel, and R. Miletich, J. Appl. Cryst. **49**, 2129 (2016).

[19] OpenSesame Documentation, `https://xweb.lanl.gov/projects/data/eos/opensesame/html_wrapper.php?documentation/index.html`.

[20] E. D. Chisholm, Tech. Rep. LA-UR-10-08329, Los Alamos National Laboratory Technical Report (2010).

[21] E. Chisholm, C. Greef, and D. George, Tech. Rep. LA-UR-05-9413, Los Alamos National Laboratory Technical Report (2005).

[22] F. D. Murnaghan, Proc. Natl. Acad. Sci. **30**, 244 (1944).

[23] F. Birch, Phys. Rev. **71**, 809 (1947).

[24] G. Ottonello, M. V. Zuccolini, and B. Civalleri, CALPHAD **33**, 457 (2009).

[25] R. J. Angel, D. R. Allan, R. Miletich, and L. W. Finger, J. Appl. Cryst. **30**, 461 (1997).

[26] NIST JANAF Thermochemical Tables, `kinetics.nist.gov/janaf`.

[27] C. T. Anderson, J. Am. Chem. Soc. **58**, 568 (1936).

[28] F. Grønvold, S. Stølen, and S. R. Svendsen, Thermochim. Acta **139**, 225 (1989).

[29] T. H. K. Barron, J. F. Collins, T. W. Smith, and G. K. White, J. Phys. C: Solid State Phys. **15**, 4311 (1982).

Appendix A: OpenSesame input files

```
! alpha quartz, low pressure phase

&job
 job_type='neweos'
 sourcelib_path='./../Library'
 resultlib_path='./../Library' /

&neweos
 material_number=90001
 material_name='solid quartz'
 author=''
 references=''
 classification='unclassified'
 composition='SiO2'
 atomic_number=10
 atomic_weight=20.028
 reference_density=2.65

 cold_model='hugfit'
 hugoniot_fit_c0=3.77
 !hugoniot_fit_s1=1.907
 hugoniot_fit_s1=1.907
 hugoniot_fit_s2=0.0

 energy_shift=0.0

 match_low=.true.
 lower_compression_cutoff=0.99
 cohesive_energy=50.
 lennard_jones_exponent=1.
 match_high=.true.
 upper_compression_cutoff=1.3
 liquid_shift=.false.
 entropy_difference=0.0

 nuclear_model='hightliq'

 reference_debye=950  ! 950?
```

```
 gruneisen_option=7

 reference_gamma=0.65
 gamma_reference_density=2.65
 gamma_at_zero=1.0
 gamma_at_infinity=0.666667
 dgamma_right=-0.65
 dgamma_left=-0.65

 melt_model='function'
 melt_option='lindemann'
 initial_melt_density=2.334
 initial_melt_temperature=1996
 electron_model='tfd'
 tfd_fix_flag=1
 elec_low_temp_interp=.true.
 ifstandard=.true.
 atmP=.false.
 hugoniot_extrap_lower=1
 hugoniot_extrap_upper=0
/

&job
 job_type='materials'
 sourcelib_path='./../Library'
 resultlib_path='./../Library'
 /

&materials
 author=''
 material_option='maxwell'
 critical_temperature=600
 critical_density=0.45
 cutoff_temperature=0.0
 maxwell_tilt_isotherms=.true.
 maxwell_tilt_fraction=1.0d-8
 source_materials=90001
 result_material=90001
 /
```

```
! stishovite-like high pressure phase

&job
 job_type='neweos'
 sourcelib_path='./../Library'
 resultlib_path='./../Library' /

&neweos
 material_number=90005
 material_name='stishovite'
 author=''
 references=''
 classification='unclassified'
 composition='SiO2'
 atomic_number=10
 atomic_weight=20.028
 reference_density=4.25

 cold_model='finite_strain'
 cold_density=4.29
 cold_bulk_modulus=300
 cold_dbdp=6.0

 fs_coeff=-500.

 energy_shift = -0.4

 match_low=.true.
 lower_compression_cutoff=0.99
 cohesive_energy=31.0
 lennard_jones_exponent=0.75
 match_high=.true.
 upper_compression_cutoff=1.5

 liquid_shift=.true.
 entropy_difference=0.8

 nuclear_model='hightliq'
```

```
 reference_debye=950

 gruneisen_option=7

 reference_gamma=1.25
 gamma_reference_density=2.65
 gamma_at_zero=1.0
 gamma_at_infinity=0.666667
 dgamma_right=-1.25
 dgamma_left=-1.25

 melt_model='function'
 melt_option='lindemann'
 initial_melt_density=2.334
 initial_melt_temperature=1996
 electron_model='tfd'
 tfd_fix_flag=1
 elec_low_temp_interp=.true.
 ifstandard=.false.
 atmP=.false.
 hugoniot_extrap_lower=1
 hugoniot_extrap_upper=0
/

&job
 job_type='materials'
 sourcelib_path='./../Library'
 resultlib_path='./../Library'
 /

&materials
 author=''
 material_option='maxwell'
 critical_temperature=100
 critical_density=2.0
 cutoff_temperature=0.0
 maxwell_tilt_isotherms=.true.
 maxwell_tilt_fraction=1.0d-8
 source_materials=90005
 result_material=90005
```

```
  /



! make the multiphase EOS

&job
 job_type='grid'
 sourcelib_path='../../Library'
/

&grid
 grid_change='copy'
 grid_type='temperature'
 grid_material=90001
 grid_table=311
/

&job
 job_type='materials'
 sourcelib_path='./../Library'
 resultlib_path='./../Library' /

&materials
 author=''
 references=''
 material_option='multiphase'
 result_material=90028
 reference_density=2.65
 nmats=2
 source_materials(1)=90001
 source_materials(2)=90005
 phase_names(1)='quartz'
 phase_names(2)='stishovite'

 make_subtables=.true.

 multiphase_flag=1
 multiphase_itmax_gp=100
```

```
 ph_rhohi(1)=5.0

 multiphase_use_311=.true. /

&job
 job_type='materials'
 sourcelib_path='./../Library'
 resultlib_path='./../Library' /

&materials
 author=''
 material_option='standardize'
 atmP=.false.
 source_materials=90028
 result_material=90028 /


&materials
 author=''
 material_option='maxwell'
 critical_temperature=100
 critical_density=2.0
 cutoff_temperature=0.0
 maxwell_tilt_isotherms=.true.
 maxwell_tilt_fraction=1.0d-8
 source_materials=90028
 result_material=90028
 /
```